

# COUPLED WAVE AND SEDIMENT DYNAMICS ON ATCHAFALAYA SHELF, LOUISIANA

Sergio Jaramillo and Alex Sheremet,

Civil and Coastal Engineering, 365 Weil Hall, University of Florida, Gainesville , FL 32611,  
USA; sjaram1@ufl.edu, alex@coastal.ufl.edu,

M. A. Allison

University of Texas Institute for Geophysics John A. and Katherine G. Jackson School of  
Geosciences, Austin, TX 78758-4445; 512-471-8453; mallison@mail.utexas.edu

## 1. INTRODUCTION

Understanding wave-sediment interaction in cohesive sedimentary environments is important for modeling sediment transport on muddy coasts. Limited field and laboratory observations have shown that waves propagating above muddy seafloors can be strongly dissipated. *Wells and Coleman (1981)* recorded more than 90% incident energy dissipation across 20-km wide shallow mudflats off the coast of Surinam; *Matthew et al. (1995)* observed 95% incident energy loss as waves crossed the 1.1 km-wide mud banks off the coast of India; mud-enhanced damping was also observed near the Mississippi Delta (*Forristall and Reece, 1985*). Laboratory studies (*Gade, 1957; Jiang and Mehta, 1995*) show 80% wave energy dissipation over a few wavelengths.

Several theoretical formulations of bed-induced wave dissipation have been proposed depending based on different mud rheology models: viscous Newtonian fluids (*Dalrymple and Liu, 1978; Ng, 2000*), surface and internal wave interaction (*Jamali et al., 2003*), visco-elasticity (*Jiang and Mehta, 1995*), visco-plasticity (*Mei and Liu, 1987*), poro-elasticity (*Yamamoto and Takahashi, 1985*), percolation (*Liu, 1973*), and others. The applicability of these models is constrained by: 1) correctly matching the hypothesized dissipation mechanism to the actual sediment type and rheological state, and 2) the condition that mud state does not change significantly over the time scales of wave evolution. Both of these constraints are challenging: identifying the rheological state in the field is technically difficult; on a more fundamental level, laboratory and (indirect) field observations (*de Wit, 1995; Sheremet and Stone, 2003; Kineke et al., 2006*) suggest that mud rheology can change “catastrophically” (i.e. over very short time scales) under energetic hydrodynamic conditions. Wave action can liquefy bottom sediment (*Chu and Foda, 1993; Foda et al., 1993*) producing Newtonian fluid or soft, unconsolidated muds with non-Newtonian behavior and significantly higher wave dissipation efficiency (*Gade, 1957*). Catastrophic mud liquefaction events have also been recorded, leading to massive submarine landslides (*Sterling and Strohbeck, 1975*).

Abandoning the assumption of steady-state bed rheology may have deeper implications than the simple requirement of using multiple wave-dissipation models. The two (perceived) separate problems of mud-induced wave dissipation and wave-induced mud state changes may have to be reformulated as a single, coupled model for wave-current-sediment dynamics over muddy sea beds.

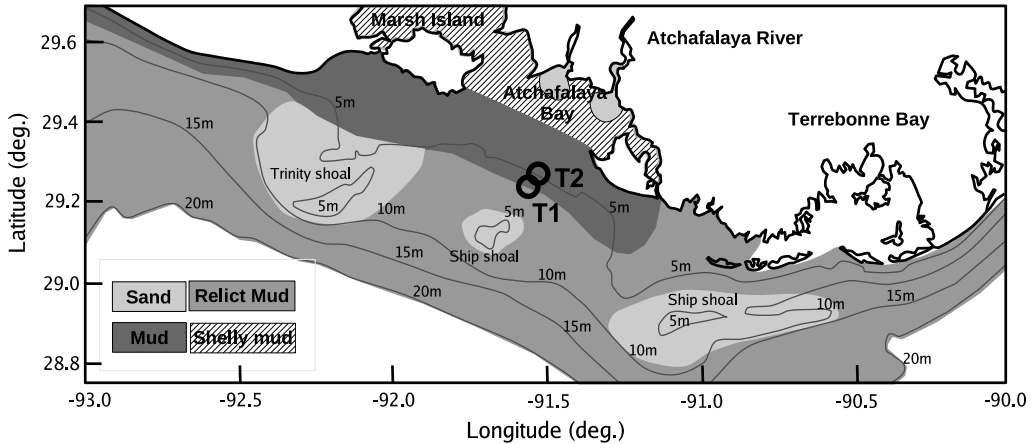


FIGURE 2.1. Facies map of the surficial sediments of the Atchafalaya inner shelf, Louisiana, USA (Neill and Allison, 2005). Relict sediment units sometimes are mantled by thin (less than 20-cm thick), ephemeral modern mud. Circles mark the location of the instrumented platforms (T1 and T2) during the 2-week experimental run of March 1-14, 2006.

To understand this coupling high-resolution and coherent field observations are needed of wave, current, and sediment dynamics. Previous field efforts have focused on either one of these processes, with a minimum of information gathered about the complementary ones. In particular, field measurements of mud rheology changes (technically challenging) are few, indirect (i.e. rheological state is inferred from general dynamical behavior) and have low time resolution (e.g. *Sterling and Strohbeck, 1975* is really a forensic analysis). Here, we present what, to our knowledge, is the first field effort to collect high resolution field observations of coupled water and sediment motion in a muddy environment. Section 2 presents briefly the field experiment, Section 3 discusses some field observations, and Section 4 summarizes the results.

## 2. FIELD EXPERIMENT

Atchafalaya Bay and shelf Figure 2.1 is an ideal location for field studies of large-scale wave propagation processes in muddy environments. An abundance of cohesive sediment is discharged in the area by the Atchafalaya River and subsequently carried to the West by prevailing winds and the Gulf of Mexico loop current. The shelf is wide and flat (almost featureless), with the 10-m isobath in some places 50 km offshore. To observe the coupling between wave and bed sediment dynamics, we deployed two instrument clusters (T1 and T2, Figure 2.1) on Atchafalaya Shelf for a duration of approximately 2 months from February through March 2006, a period in the year typically characterized by the energetic waves and high river discharge. The experiment was sectioned into 2-week runs interrupted by breaks for instrument maintenance and data downloading. Several experimental sites and cluster configurations were used, all located in the vicinity of the 5-m isobath. The data presented here were collected using a deployment configuration nearly parallel to the local bottom gradient (cross-shore, T1 located about 4 km offshore of T2) in the 2-week window of March 1-14, 2006.

The list of instruments used (in both T1 and T2) includes a high-resolution, downward-looking Sontek PC-ADP (pulse-coherent acoustic Doppler profiler) and an upward-looking RDI ADCP (acoustic Doppler current profiler). The PC-ADP provided high-resolution information of water and sediment motions in the first 50 cmab by sampling pressure and three-dimensional current velocity at 2 Hz, in 17 bins 3-cm high, continuously for the entire duration of a 2-week run. The ADCP measured current and directional wave motions in the upper water column in 30-cm bins. Pressure was measured continuously at 2 Hz using a redundant array of pressure sensors (one independently logged and one on each of the profilers), located at approximately 1 mab. Near-bed sediment dynamics was monitored using OBS (optical backscatterance sensors) located at 0.3 and 1 mab. A pencil-beam 600-kHz ABS (acoustic backscatter sensor) was used to monitor the position of the bottom and strata formation. At this frequency the ABS signal can penetrate the lutocline and provide clear image of the evolution of fluid-mud layers. Not all the instruments were deployed at any one moment, and some were available only later in the experiment, e.g. a Sequoia Scientific LISST (system for in-situ measurement of particle size and distribution) was deployed at T2 in the last 2-week run at the end of March 2006.

### 3. OBSERVATIONS

Figure 3.1 shows a summary of wind, wave, and tide conditions observed at T1 during the March 1-14 deployment period. A quasi-stationary cold front moved slowly over the observation area through March 8-13, generating steady winds of 10-15 m/s and at the peak of the storm waves of almost 2-m height (Figure 3.1a). The storm did not distort significantly the tidal elevation signal (typically less than 1-m range, Figure 3.1b,c); however, velocity profiles observed by the T1 ADCP show wind-forced tidal currents oscillating in the N-NW direction with less significant southward flow(Figure 3.1c).

Figure 3.2 compares observed near-bottom velocity distribution to the raw sonar return intensity values (not corrected for attenuation due to suspended sediment). Short waves (seas) were fairly responsive to local wind forcing, reaching about 1-m height as soon as the wind picked up (Figure 3.2a, also Figure 3.1a). Swell developed and arrived later, with a relatively steady direction, correlated with the dominant fetch direction approximately with the South-North axis. Throughout the March 8-13 storm, the dominant wave direction for both sea and swell was toward N-NW. At the peak of the storm swell reached heights of up to 1-m with a peak period of about 10 s. Band significant height is defined here based on the first spectral moment  $H_{sig} = 4\sqrt{\int_{f_1}^{f_2} S(f)df}$ , where  $S(f)$  is the spectral density of wave variance,  $f$  is the frequency, and the integration limits are the limits of the frequency bands ( $f_0 = 0.05$  Hz,  $f_1 = 0.2$  Hz for swell;  $f > 0.2$  Hz for swell).

The acoustic instruments pointed downward (PC-ADP and ABS) provided indirect observations of sediment dynamics. The response of bed sediment to wave-current activity can be inferred by comparing two independent estimates of bottom position: maximum echo intensity, indicating the location of the strongest reflection surface (white line in Figure 3.2d) and zero-velocity level, the hydrodynamic bottom (red line, Figure 3.2c) based on the observed vertical structure of near-bed velocity. The two curves are copied in panels 3.2b,c, and d. In the absence of suspended sediment, the strongest-reflection surface should be identified as the bed, since maximum return intensity is associated with the strongest vertical gradient of density. The two independent estimates agree within a 3 cm (one PC-ADP bin height) error during the pre- and post-frontal stages, March 7 to

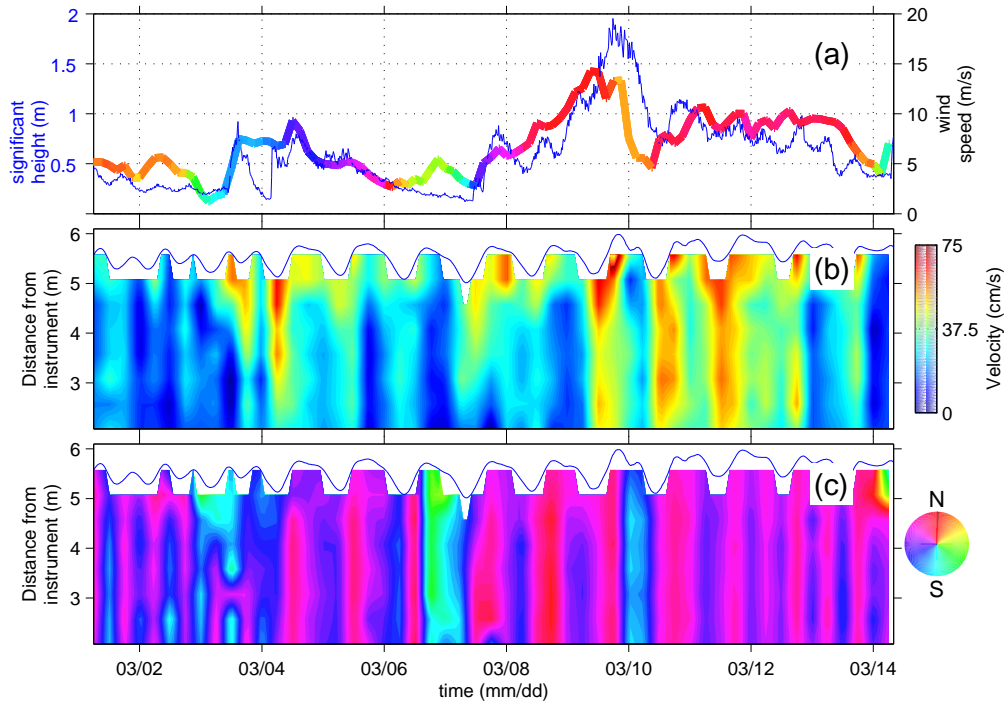


FIGURE 3.1. Wave, wind and current profile measurements at T1 (circles, Figure 2.1) during the storm of March 8-13, 2006. a) Significant wave height from the ADCP; wind intensity and direction; b-c) vertical distribution of current velocity magnitude (20 min averages) and direction, measured by the ADCP. The blue line represents the mean free surface elevation. Directions given here are flow direction (e.g. North means flowing toward North).

evening of March 9, and March 12 and on, respectively. However, there are two occurrences of about one-day each (evening of March 9 – evening of March 10; and March 11), corresponding to the two peaks of swell activity, when the two estimates disagree, with the strongest-reflection surface about 10-15 cm higher than the hydrodynamic bottom. A mobile (velocities up to about 30 cm/s) and dense layer of sediments formed during these events, consistent with what could be called fluid muds. The strongest-reflection surface could be identified as the lutocline during these events.

The changes in the vertical structure of the near-bed velocity field and bed-elevation suggest that the two fluid-mud events may have distinct characters. The first event is associated with the increase of swell energy (from 1 to 1.5 m height) as the front approaches the observation site and is consistent with a liquefaction/resuspension process. The direction (southward) of flow within the layer is similar to the flow of the rest of the water column flow; during this event the instrument platform sank into the bed by about 10 cm.

The second fluid-mud event occurs in the wake of the front, under less intense wave action (swell height of about 0.8 m); the mud layer appears to be less mobile (velocity up to about 20 cm/s); the layer flows southward, opposite to the direction of the flow in the rest of the water column; no further sinking of the platform is observed. These characteristics are consistent with a sediment

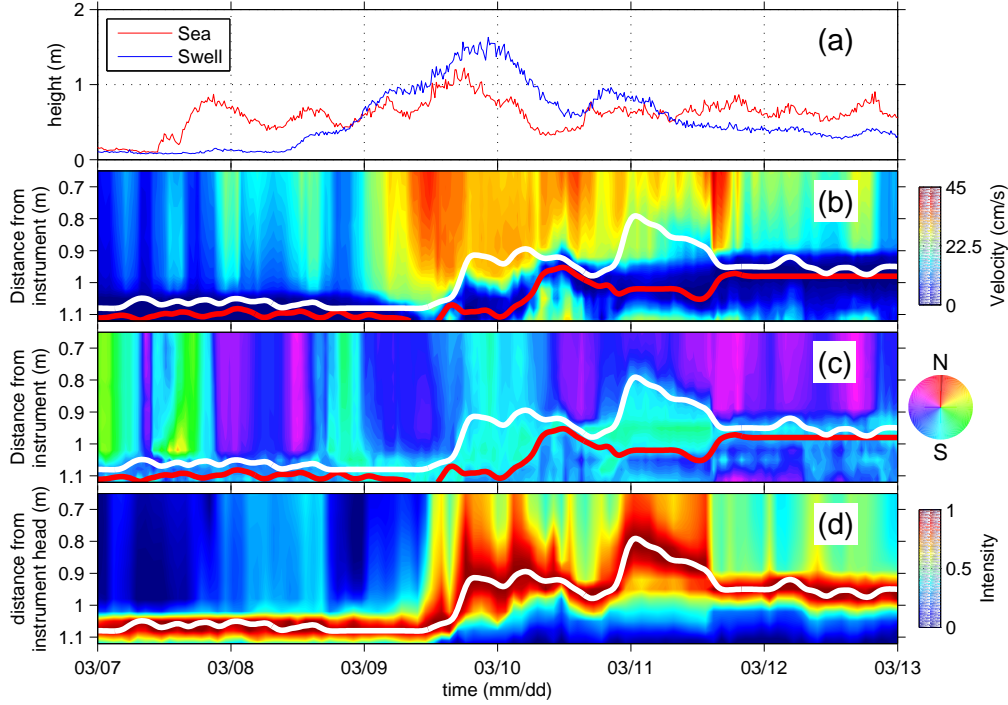


FIGURE 3.2. PC-ADP observations of fluid mud formation during the storm of March 8-13 2006. Deployment configuration is shown in Figure 2.1 (circles). a) Wave heights (blue/dark line – swell,  $0.05 \text{ Hz} \leq f < 0.2 \text{ Hz}$ ; red/light line – seas,  $f \geq 0.2 \text{ Hz}$ ); b) Velocity profile, magnitude; c) Velocity profile, direction; d) Signal return intensity. On panels b-d the estimated locations of bottom position are plotted (white line – strongest-reflection surface; red line – zero velocity position).

settling/advection mechanism, maybe similar to gravity flows observed on the shelf fronting Eel River (Traykovski *et al.*, 2000).

The response of the wave field to changes in the bed structure is illustrated in Figure 3.3. The convenient (arbitrary) division into swell and sea frequency bands is suggested by evolution of the wave spectrum observed at T1 (Figure 3.3a). Short waves (seas) characteristic of low energy conditions typically occupy the frequency band above 0.2 Hz; swells with frequencies lower than 0.2 Hz propagate into the area only during the March 8-13 storm, when the peak of the spectrum goes as low as 0.1 Hz., and infragravity waves are also generated. Figure 3.3c shows the PC-ADP return intensity signal, together with the estimated position of the bottom/lutocline. The peaks on March 10-11 represent the two fluid-mud events discussed above. Figure 3.3b shows the evolution of wave transmission from T1 to T2, estimated as the fraction of swell variance at T1 that reaches T2

$$(3.1) \quad \text{net swell variance transmission} = \frac{\int_{f_1}^{f_2} S_2(f) df}{\int_{f_1}^{f_2} S_1(f) df},$$

where  $S_{1,2}(f)$  is the spectral density of variance estimated at T1 and T2 respectively, and the integration is done over the swell band defined as before,  $0.05 \text{ Hz} = f_1 < f \leq f_2 = 0.2 \text{ Hz}$ . Expression (3.1) lumps together the effects of all variance-altering processes (e.g. mud-induced dissipation,

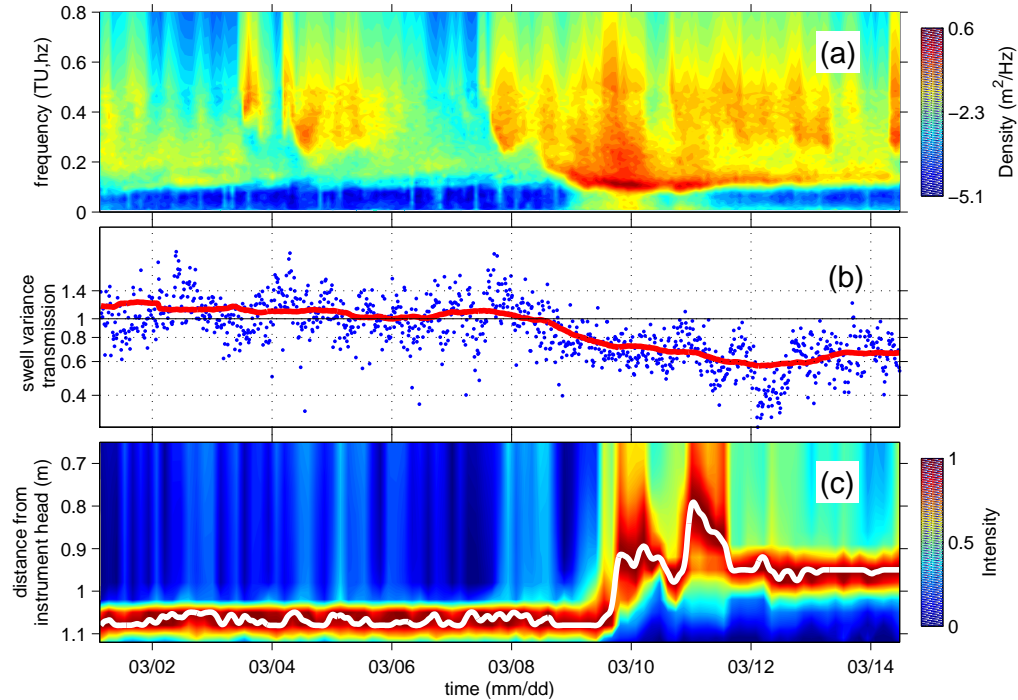


FIGURE 3.3. Swell response to bottom processes preceding and during the storm of March 8-13, 2006. a) Evolution of the wave spectrum at T1; b) swell variance transmission between T1 and T2 (fraction of swell variance recorded at T1 that reaches T2); c) PC-ADP return signal intensity, versus time. On panel b) blue points represent values computed using 20-min estimates of variances; the red curve is a 2-day moving average, given here to highlight the general trend of transmission evolution. On panel c) the white line marks the location of the maximum reflecting surface (.

whitecapping, wind generation, nonlinear interactions, and others); however, numerical simulations (not shown) suggest that wave-bottom interaction is the dominant mechanism, with other processes having negligible effects. We will assume in the sequel that Figure 3.3b represents with a good approximation the dissipative effects of wave-bottom interaction.

Hourly transmission values (blue dots in Figure 3.3b) are fairly noisy and show obvious tidal modulation. Some of the noise might be due to directional variability and low swell energy. Throughout this dataset swell direction is roughly in the N-NW band; estimates are less noisy for higher energy swell (e.g. March 10-12), which typically also have much narrower (about 5 degrees) directional spread. Tides modulate transmission by modifying near-bed orbital velocity (depth fluctuations – velocity increases at low tides) and through coupling between wave motion and oscillating tidal circulation. These effects are being studied and the results will be reported elsewhere.

A 2-day moving average of the transmission estimate that eliminates noise and tides (red line, Figure 3.3b) is shown to highlight the trends in the evolution of swell transmission. Overall, it suggests a strong correlation between swell dissipation and swell energy. Net transmission values average close to 1 during low swell energy periods (e.g. March 1-8, with 10-15 cm height, also Figure 3.2a) and begin to drop as soon as swell energy increases (March 9) reaching a minimum

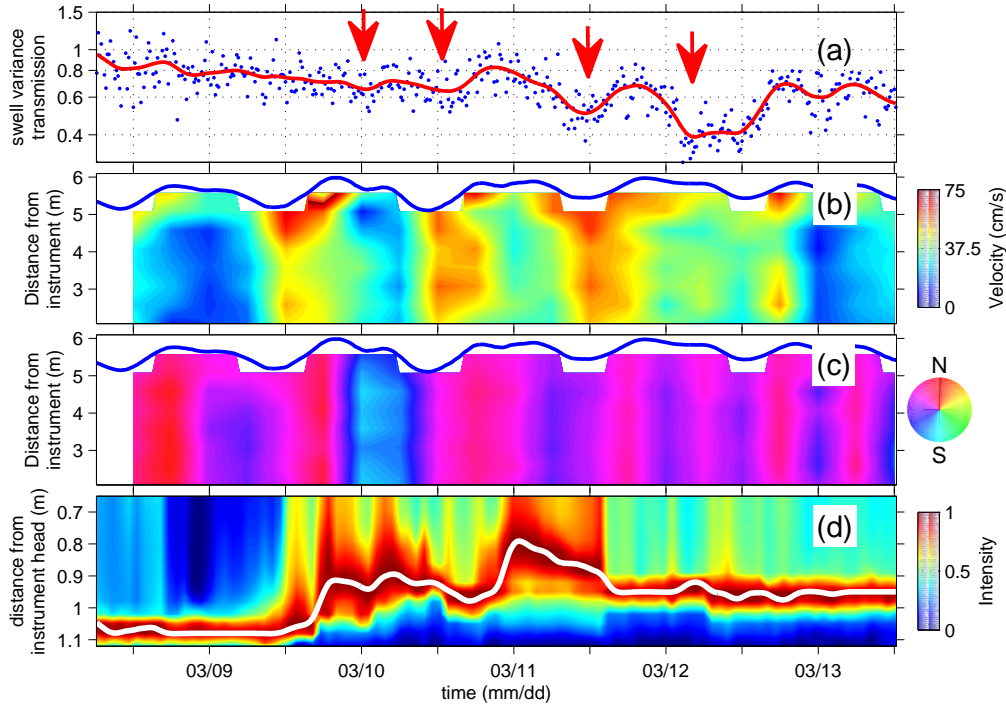


FIGURE 3.4. Detail of wave and sediment observations collected at T1 during the peak and waning phase of the March 8-13. a) Swell variance transmission between T1 and T2; b-c) vertical profile of velocity magnitude and direction measured by the ADCP; d) return signal intensity (PC-ADP), versus time. Red line on panel a) is a short-time moving average; arrows mark the low transmission events. All but the last such event appear to be correlated well with tidal lows.

of about 0.6 toward the end of the storm. Figure 3.4 compares in more detail the modulation of the wave transmission signal to tides and bottom sediment response. Surprisingly, the two fluid mud events (two peaks of the white line in Figure (3.4)d, also Figure (3.2)b-d) do not have a clear effect on swell dissipation. Three weak transmission minimum on March 10-11 that coincide with these events appear to be correlated to low tides and might be due to tidal modulation. However, the sharp decrease on March 12 (last arrow in Figure 3.4a) corresponds overall to high tide conditions, and occurs one day after the last fluid-mud observation.

Several arguments can be offered to explain the weak impact of fluid-mud events on swell dissipation. The observed fluid-mud events seem to have been produced by two different mechanisms and maybe have different characteristics (density, viscosity, floc size, and so on); the fluid-mud layers may just not be dense enough to extract much energy from the waves; they may not blanket enough area between the two observation sites to produce noticeable accumulated effects. Direct measurements of suspended sediment concentration in high-density suspensions are at best difficult and our experiment had no instrument with such capability. In addition, our data represent two points separated by a 4 km distance. It is impossible to estimate the spatial extent of these the fluid-mud layers. Even on a flat and featureless shelf, it is likely that fluid-mud layers form and flow in a

fingering-like pattern that might cover a small overall area on the bottom. In fact, examination of the T2 data shows no signs of the fluid muds seen at T1.

The continuous increase in swell dissipation in the wake of the storm (0.4 transmission attained on March 12) is puzzling. A possible explanation might be that wave action during the storm liquefied and softened the bottom for a depth larger than the few centimeters suggested by the settling of the instrument platform. This effect would happen over a larger area than just the one covered by fluid muds and the slow consolidation process would extend beyond the period of high wave activity, enhanced by sediment settling in the wake of the storm. Cores taken at the end of this period support this hypothesis; the analysis of some of the data sets collected is ongoing.

#### 4. SUMMARY

Our field observations of wave-current-sediment interaction in muddy environments suggest that sediments respond to changes in the sea state on temporal and spatial scales similar to those characteristic of wave-current evolution. To our knowledge, this is the first time high spatial and temporal resolution measurements support this hypothesis. During an energetic storm, we identified two fluid mud layer events. Our analysis suggests that the processes leading to their formation differ: one may be associated with bed liquefaction, the other with advected fluid muds possibly in the form of gravity flows.

The estimate discussed for wave dissipation lumps together the effects of all processes that can modify wave variance; the signal is noisy and modulated by tides. A clear correlation between swell energy and dissipation efficiency can be observed in the averaged signal, with wave dissipation increasing as swell energy increases. We expected fluid-mud events to have a strong dissipative effects on wave propagation. Surprisingly, our data show no significant dissipative effects associated with the occurrence of fluid muds. Rather, a maximum swell dissipation is observed well after the fluid muds must have settled, suggesting that the most-dissipative mud state in the study area might be the soft mud phase associated with sediment de-watering and consolidation process.

#### ACKNOWLEDGMENTS

The work presented here was supported by the Office of Naval Research Contracts N00014-07-1-0448 and N00014-07-1-0607. Field data was collected with support by the Field Support Group in the Coastal Studies Institute, Louisiana State University, lead at the time by Captain Steve Dartez.

#### REFERENCES

- Chou, H.-T., M.A. Foda, and J.R. Hunt, Rheological response of cohesive sediments to oscillatory forcing, In: *Nearshore and Estuarine Cohesive Sediment transport*, Coastal Estuarine Sci., 42, A.J. Mehta ed., p. 126-148, AGU, Washington DC, 1993.
- Dalrymple, R.A. and P.L.-F Liu, Waves over soft muds: a two-layer fluid model, *J. Phys. Oceanogr.* 8, p. 1121-1131, 1978.
- De Wit, P.J., Liquefaction of cohesive sediment by waves. PhD-dissertation. Delft University of Technology, The Netherlands, 1995.
- Foda, A.M., J.R. Hunt, and H.-T. Chou, A nonlinear model for the fluidization of marine mud by waves, *J. Geophys. Res.*, 98, 7039-7047, 1993.
- Forristall, G.Z., and A.M. Reece, 1985. Measurements of wave attenuation due to a soft bottom: the SWAMP experiment, *J. Geophys. Res.*, 90(C2), 3367-3380, 1985.

- Gade, H. G., Effects of a non-rigid impermeable bottom on plane surface waves in shallow water, PhD Thesis, 35pp., Texas A&M Univ., College Station, Tex., 1957.
- Jamali, M., B. Seymour, and G. Lawrence, Asymptotic analysis of a surface- interfacial wave interaction, *Phys. Fluids* 15, 47-55, 2003.
- Jiang F. and A.J. Mehta, Mudbanks of the Southwest Coast of India IV: Mud viscoelastic properties, *J. Coastal Res.*, 918–926,1995.
- Kineke, G.C., E.E. Higgins, K.Hart, D. Velasco, Fine-sediment transport associated with cold front passages on the shallow shelf, Gulf of Mexico, *Cont. Shelf. Res.*, 26, 2073-2091, 2006.
- Liu, P. L.-F., Damping of water waves over porous bed. *J. Hydraulics Div.*, ASCE, 99(12): 2263-71, 1973.
- Mathew J., M. Baba, and N. Kurian, Mudbanks of the Southwest coast of India I: Wave characteristics. *J. Coastal Res.*, 11, 168-178, 1995.
- Mei, C.C., and Liu, K.F., A Bingham Plastic Model for a Muddy Seabed Under Long Waves, *J. Geophys. Res.*, 92(C13):14581-14594, 1987.
- Neill, C.F. and Allison, M.A., Subaqueous deltaic formation on the Atchafalaya Shelf, Louisiana. *Marine Geology*, 214:411-430, 2005.
- Ng, C.-O., 2000. Water waves over a muddy bed: a two-layer Stokes' boundary layer model. *Coast. Eng.*, 40, 221–242.
- Sheremet, A. and G.W. Stone, Observations of nearshore wave dissipation over muddy sea beds, *J. Geophys. Res.*, 108, C11, doi: 10.1029/2003JC001885, 2003.
- Mathew J., M. Baba, and N. Kurian, Mudbanks of the Southwest coast of India I: Wave characteristics. *J. Coastal Res.*, 11, 168-178, 1995.
- Sterling, G.H., and G.E. Strohbeck, Failure of South Pass 70 Platform B in Hurricane Camille, *J. Pet. Tech.*, 27, p. 263-268, 1975.
- Traykovski, P., W. R. Geyer, J. D. Irish, and J. F. Lynch, The role of wave-induced density-driven fluid mud flows for cross-shelf transport on the Eel River continental shelf, *Continental Shelf Research*, 20, p.: 2113-2140, 2000.
- Wells, J. T. and Coleman J. M., Physical processes and fine-grained sediment dynamics, coast of Suriname, South-America, *J. of Sedim. Petrology.*, 51 (4): 1053-1068, 1981.
- Yamamoto T., and S. Takahashi, Wave damping by soil motion, *ASCE J. of Waterway, Port, Coast., and Ocean Eng.*, 111, 1, 62–77, 1985.